

Supporting Information for

Bimetallic Nickel Cobalt Sulfide as Efficient Electrocatalyst for Zn-Air Battery and Water Splitting

Jingyan Zhang^{1, ‡}, Xiaowan Bai^{2, ‡}, Tongtong Wang¹, Wen Xiao³, Pinxian Xi⁴, Jinlan Wang², Daqiang Gao^{1, *}, John Wang^{3, *}

¹Key Laboratory for Magnetism and Magnetic Materials of MOE, Key Laboratory of Special Function Materials and Structure Design of MOE, Lanzhou University, Lanzhou 730000, People's Republic of China

²School of Physics, Southeast University, Nanjing 211189, People's Republic of China

³Department of Material Science and Engineering, National University of Singapore, Engineering Drive 3, 117575, Singapore

⁴Key Laboratory of Nonferrous Metal Chemistry and Resources Utilization of Gansu Province and The Research Center of Biomedical Nanotechnology, Lanzhou University, Lanzhou 730000, People's Republic of China

*Corresponding authors.

Email: gaodq@lzu.edu.cn (Daqiang Gao); msewangj@nus.edu.sg (John Wang)

‡Both authors contribute equally to this work

S1 Materials Characterizations

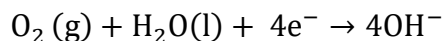
The crystal structure of each sample was studied by using X-ray diffraction for phase analysis (XRD, X' Pert PRO PHILIPS with Cu K α radiation). X-ray photoelectron spectroscopy (XPS, Kratos Axis Ultra) was conducted to study the elementary composition and the bonding characteristics in each sample. The morphology and high-resolution images were characterized using scanning electron microscopy (SEM, Hitachi S-4800) and transmission electron microscopy (TEM, TecnaiTM G2 F30, FEI, USA). Raman spectra were acquired using a Jobin-Yvon LabRam HR80 spectrometer (Horiba Jobin Yvon, Inc.) with 532 nm line of Torus 50 mW diode-pumped solid-state laser under backscattering geometry. Electrochemical measurements were performed in a standard three-electrode electrochemical cell using an electrochemical workstation (CHI660e).

S2 Preparing of Glassy Carbon Electrode and Rotating Ring-Disk Electrode

The electrode liquid is coated to glassy carbon electrode or rotating ring-disk electrode with a pipette with a capacity of 0.2 mg cm^{-2} . The coated electrode were let dried in air before test.

S3 Calculation Details

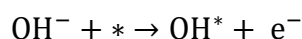
The DFT calculations were performed by Vienna ab initio simulation package (VASP). The standard generalized-gradient approximation (GGA) in the form of the Perdew-Burke-Ernzerhof (PBE) exchange model was used. The energy cutoff for the plane-wave basis set and the convergence threshold to obtain the wave functions were 400 eV and 10^{-5} eV, respectively. 3d electrons of Ni was treated using the GGA+U method with the U_{eff} (U-J) of 5.76 eV. Ionic relaxations were conducted until all force components became $<0.02 \text{ eV \AA}^{-1}$. For the density of states (DOS), the Brillouin zone is represented by the set of $5 \times 5 \times 5$ k points for the geometry optimizations. A rectangular supercell with $11.00 \text{ \AA} \times 11.00 \text{ \AA}$ was used to calculate the OER activity with the active site on (100) surface. In alkaline environment, the standard oxygen reduction reaction is described as follow [S1]:



$$E^0 = 0.402 \text{ V}$$

Four steps are involved in the OER performance, the corresponding Gibbs free energy (G) was valued via the following mechanism:

Step 1:



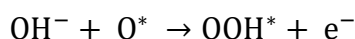
$$\Delta G_1 = [(E_{\text{DFT}}^{\text{OH}^*} + \text{ZPE} - TS^0) - E_{\text{DFT}}^*] + 9.952 \text{ Ev}$$

Step 2:



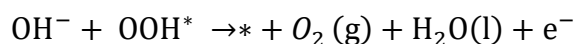
$$\Delta G_2 = [(E_{\text{DFT}}^{\text{O}^*} + E_{\text{DFT}}^{\text{H}_2\text{O}(\text{g})}) - E_{\text{DFT}}^{\text{OH}^*} + (\Delta\text{ZPE} - TS^0)] + 9.952 \text{ Ev}$$

Step 3:



$$\Delta G_3 = [(E_{\text{DFT}}^{\text{OOH}^*} - E_{\text{DFT}}^{\text{O}^*}) + (\Delta\text{ZPE} - TS^0)] + 9.952 \text{ Ev}$$

Step 4:



$$\Delta G_4 = (E_{\text{DFT}}^* + (4.92 + 2(E_{\text{DFT}}^{\text{H}_2\text{O}(\text{g})} - E_{\text{DFT}}^{\text{H}_2(\text{g})}) + E_{\text{DFT}}^{\text{H}_2\text{O}(\text{g})}) - E_{\text{DFT}}^{\text{OOH}^*} + (\Delta \text{ZPE} - TS^0) + 9.952 \text{ eV}$$

The Gibbs free energy (G) for OER is

$$G^{\text{OER}} = \max[\Delta G_1^0, \Delta G_2^0, \Delta G_3^0, \Delta G_4^0]$$

The theoretical onset overpotential is

$$\eta = \max[\Delta G_1^0, \Delta G_2^0, \Delta G_3^0, \Delta G_4^0]/e - 0.402 \text{ V}$$

Where ZPE is zero point energy and TS is entropic contributions (TS) to the free energies.

S4 HER Measurements

In the standard three-electrode electrochemical cell of electrochemical workstation (CHI660e), graphite electrode, Ag/AgCl, and glassy carbon electrode were used as the counter, reference, and working electrode. All the data were recorded at a sweep rate of 5 mV s^{-1} after applying a number of cyclic voltammetric scanings until they were stable. Current density was normalized to the geometrical area of the working electrode. The electrochemical measurements were iR -corrected until otherwise specified. The potential of Ag/AgCl is related to RHE by the equation of $E(\text{RHE}(\text{V})) = E(\text{Ag}/\text{AgCl}) + 0.197 \text{ V} + 0.059 \cdot \text{pH}$.

S5 OER Measurements

For OER characterization, the typical process is similar to that of HER, except that the test was conducted in an alkaline electrolyte 0.1 M KOH .

S6 ORR Measurements

The catalyst ink was pipetted onto the disk electrode or ring disk electrode to obtain a catalyst loading of 0.2 mg cm^{-2} , which was used to test for ORR. Electrochemical experiments were carried out in O_2 -saturated 0.1 M KOH electrolyte for ORR. The potential range is cyclically scanned between 0.2 and 1.0 V vs. RHE with a scan rate of 2 mV s^{-1} . The CV and LSV were obtained at the ambient temperature after purging with O_2 or N_2 gas for 30 min . The potential cycling was repeated until stable voltammogram curves were obtained. RDE measurements were made at rotating rates varying from 400 to 2400 rpm , at a scan rate of 2 mV s^{-1} .

Kinetic parameters were obtained on the basis of the following Koutecky–Levich (K-

L) equation:

$$1/j=1/j_k+1/(B\omega^{1/2})$$

B , the slope of K - L plot, can be obtained from the following:

$$B=0.2 nF(D_{O_2})^{2/3}\nu^{1/6}C_{O_2}$$

where j is the measured current density, j_k is the kinetic current density, ω is the rotation speed (the constant of 0.2 is used when the rotation speed is expressed in rpm), n is the electron transfer number, F is the Faraday constant (96485 C mol^{-1}), C_{O_2} is the saturated concentration of O_2 in the electrolyte ($1.21 \times 10^{-6} \text{ mol cm}^{-3}$), D_{O_2} is the diffusion coefficient of O_2 in 0.1 M KOH solution ($D_{O_2}=1.9 \times 10^{-5} \text{ cm}^2 \text{ s}^{-1}$), ν is the kinetic viscosity of the electrolyte ($0.01 \text{ cm}^2 \text{ s}^{-1}$).

S7 Zn–air Batteries

Home-made electrochemical cells of rechargeable Zn–air battery are constructed in the present work. The active material, made as detailed in the experimental procedure, was coated on carbon paper substrate as the air cathode. A polished Zn plate was employed as the anode, and a 6 M KOH + 0.2 M Zn(Ac)₂ aqueous solution was utilized as the electrolyte. Battery tests were performed at room temperature using a LAND CT2001A instrument. In the cycling test, one cycle typically consists of one discharging step (2 mA cm^{-2} for 5 min) followed by one charging step of the same current density and duration time.

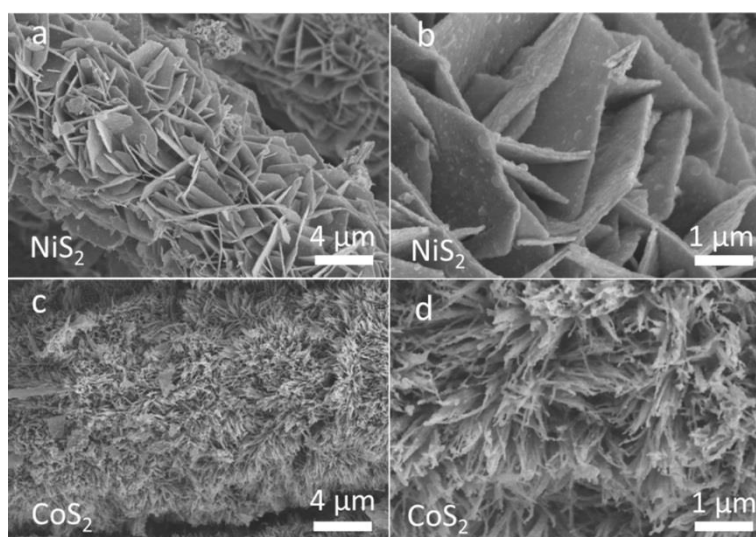


Fig. S1 **a** Low-magnification, and **b** high-magnification SEM image of NiS_2 . **c** Low-magnification and **d** high-magnification SEM image of CoS_2

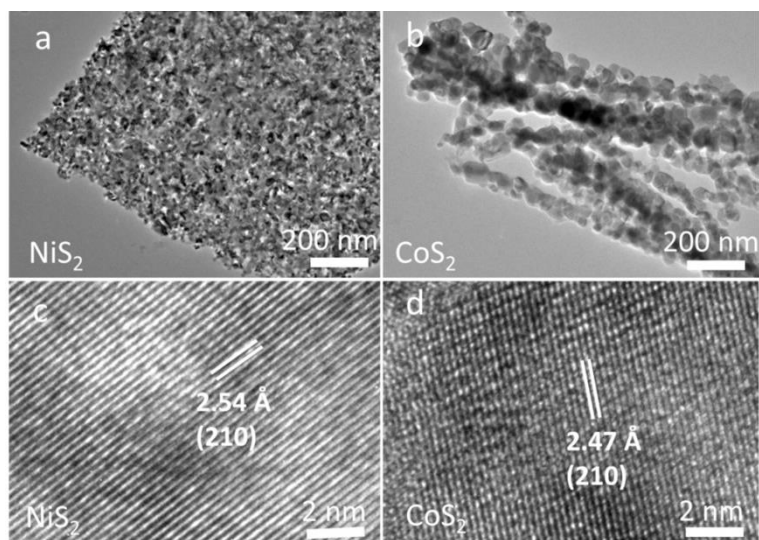


Fig. S2 TEM images of **a** NiS₂, and **b** CoS₂. High resolution TEM images of **c** NiS₂ and **d** CoS₂

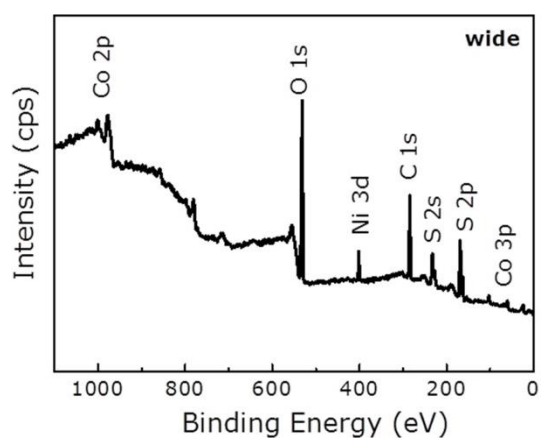


Fig. S3 The wide spectrum of XPS of (Ni,Co)S₂

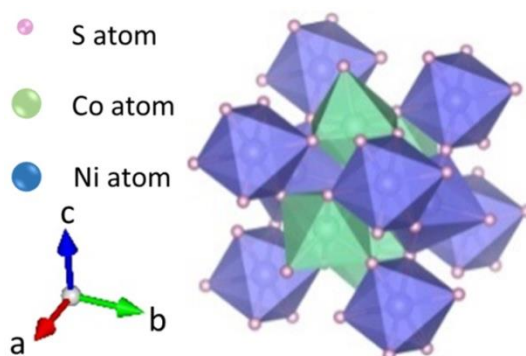


Fig. S4 Schematic diagram of atomic structure of (Ni,Co)S₂

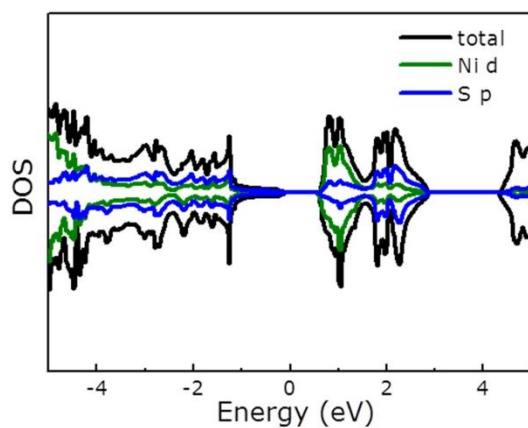


Fig. S5 Calculated partial density of states (PDOS) result for NiS₂

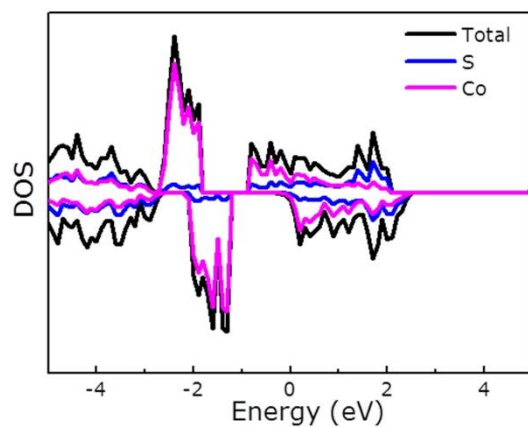


Fig. S6 Calculated partial density of states (PDOS) result for CoS₂

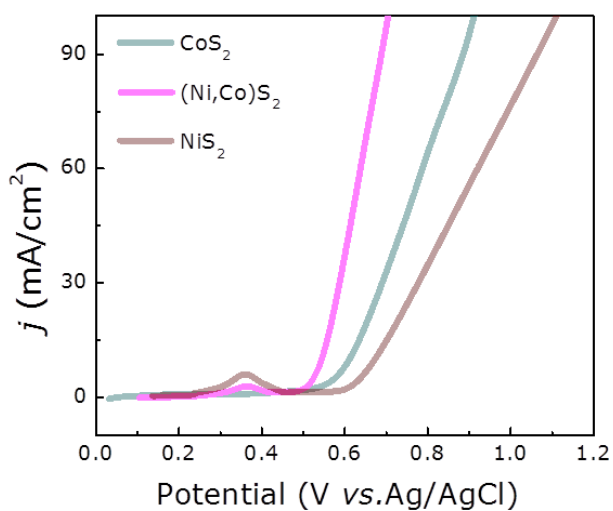


Fig. S7 Linear voltammetry scanning (LSV) curves (vs. Ag/AgCl) of (Ni,Co)S₂, NiS₂, CoS₂ and Ir/C (20% Ir) at 5 mV/s in 0.1 M KOH

S8 Calculation of Effective Active Surface Area (ECSA)

The double layer capacitance (C_{dl}) is obtained by cyclic voltammetry at different scan rates (in the range of 20~180 mV s^{-1}) to be linearly proportional to effective active surface area (ECSA). The potential is in the range from 0.2 to 0 V vs. Ag/AgCl, the C_{dl} is estimated by plotting the difference between anodic and cathodic currents ($j_a - j_c$) at 0.1 V vs. Ag/AgCl against various scan rates, where the slope is double C_{dl} . The specific capacitance C_{dl} can be converted into an electrochemical active surface area (ECSA) using the specific capacitance value for a flat standard with 1 cm^2 of real surface area. The specific capacitance for a flat surface is generally found to be in the range of 20-60 $\mu\text{F cm}^{-2}$ [S2]. In the following calculations of ECSA we assume 40 $\mu\text{F cm}^{-2}$,

$$\text{ECSA} = \frac{C_{dl}}{40 \mu\text{F cm}^{-2} \text{ per cm}^2_{\text{ECSA}}}$$

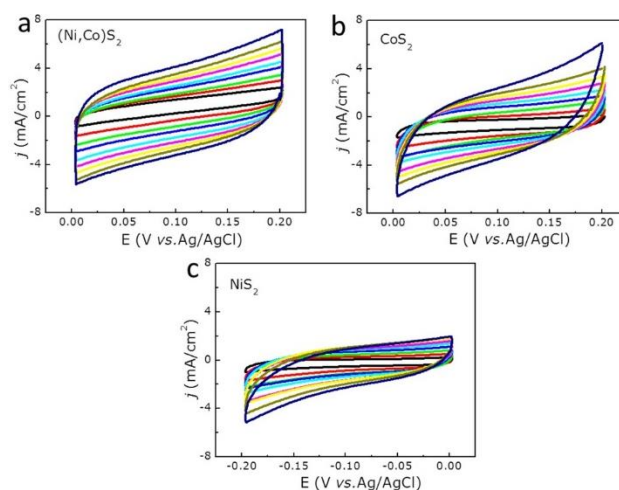


Fig. S8 CV curves of **a** (Ni,Co)S₂, **b** CoS₂ and **c** NiS₂ in 0.1 M KOH solution

S9 Turnover Frequency (TOF) in OER Calculation [S3]

The TOF values were calculated by assuming that every metal atom is involved in the catalysis:

$$\text{TOF} = jS/(4Fn)$$

Here, j (mA cm^{-2}) is the measured current density, S is the surface area of the electrode, the number 4 means 4 electrons per mol of O₂, F is the Faraday's constant (96,485 C mol^{-1}) and n is the moles of coated metal atom on the electrode.

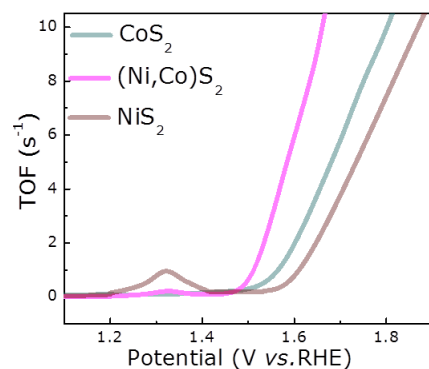


Fig. S9 The OER TOF results of (Ni,Co)S₂, NiS₂ and CoS₂

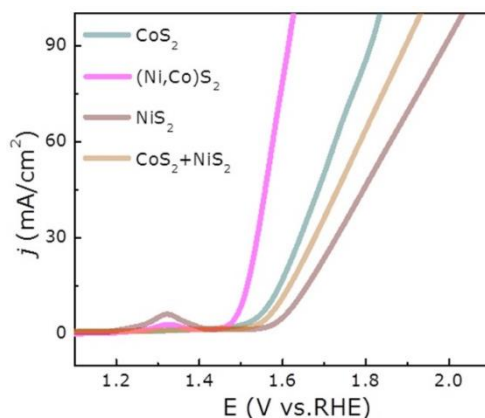


Fig. S10 Polarization curves of (Ni,Co)S₂, NiS₂, CoS₂ and (CoS₂+NiS₂) at 5 mV s⁻¹ in 0.1 M KOH

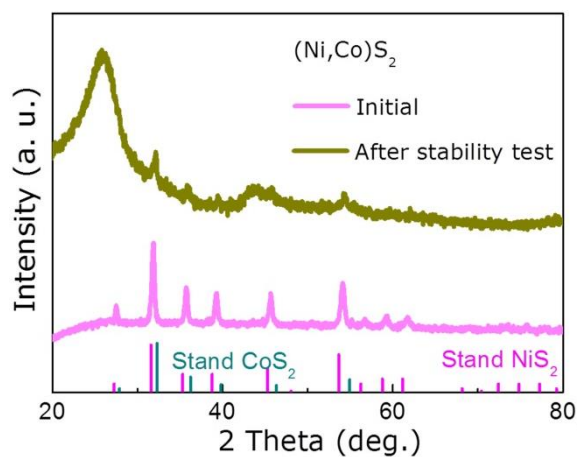


Fig. S11 XRD patterns of (Ni,Co)S₂ at the initial stage and after the stability test

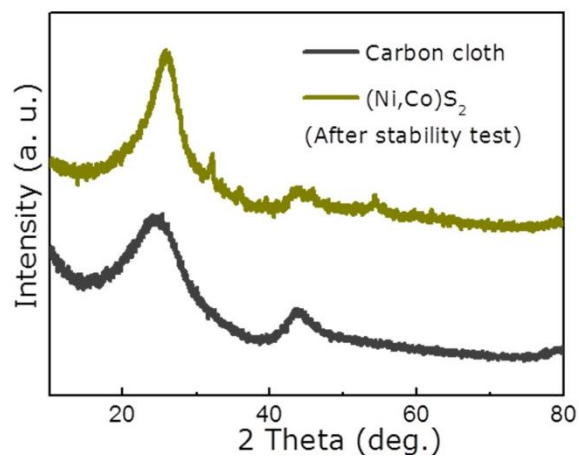


Fig. S12 XRD patterns of carbon cloth, and (Ni,Co)S₂ after the stability test

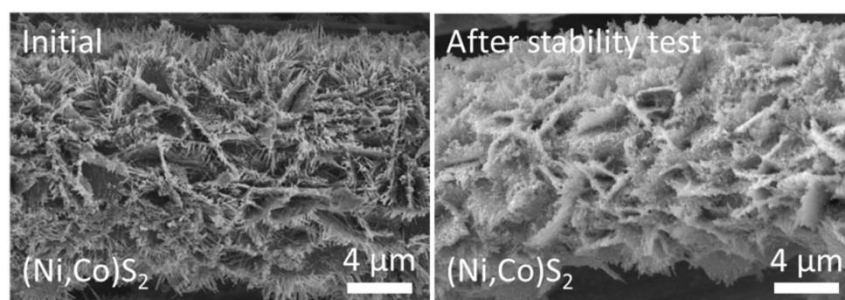


Fig. S13 SEM image of **a** initial, and **b** after the stability test of (Ni,Co)S₂

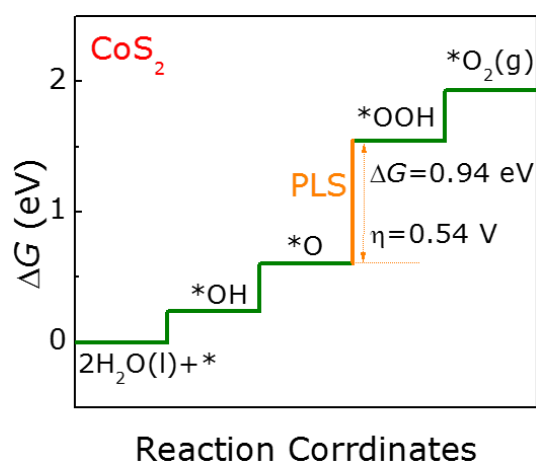


Fig. S14 Schematic of the Gibbs free energy changes for the four elementary steps during the OER on CoS₂ (100) surface

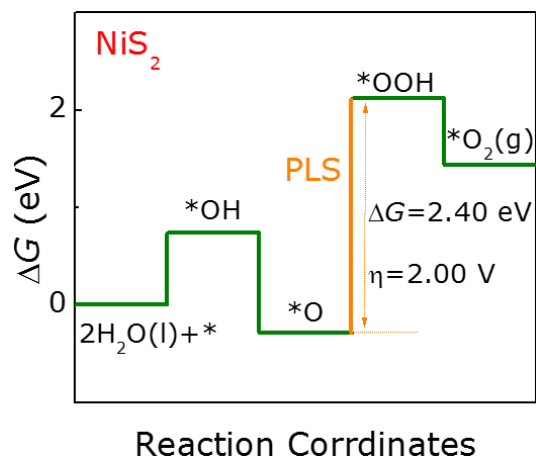


Fig. S15 Schematic of the Gibbs free energy changes for the four elementary steps during the OER on NiS₂ (100) surface

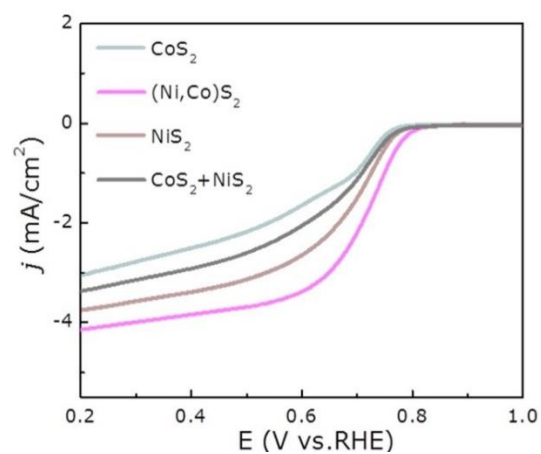


Fig. S16 ORR polarization curves of (Ni,Co)S₂, NiS₂, CoS₂ and (CoS₂+NiS₂) at 2 mV s⁻¹ in 0.1 M KOH at 1600 rpm

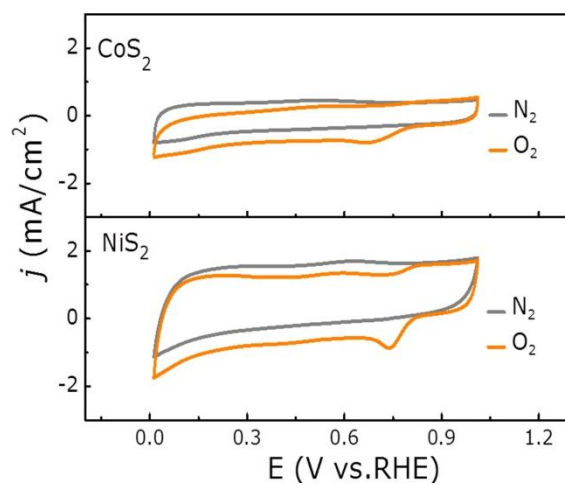


Fig. S17 CVs of NiS₂ and CoS₂ in O₂ and N₂-saturated 0.1 M KOH solution

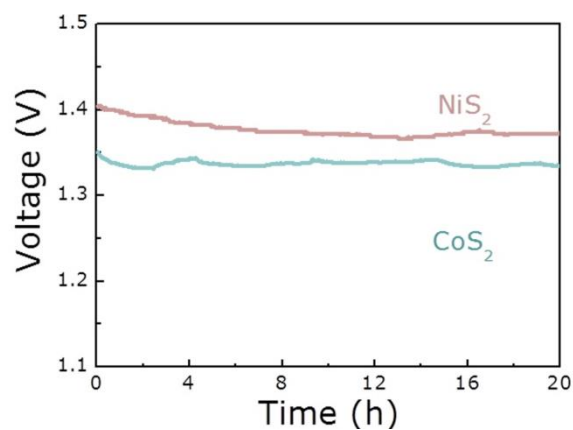


Fig. S18 Open cell voltage curves of of NiS₂ and CoS₂

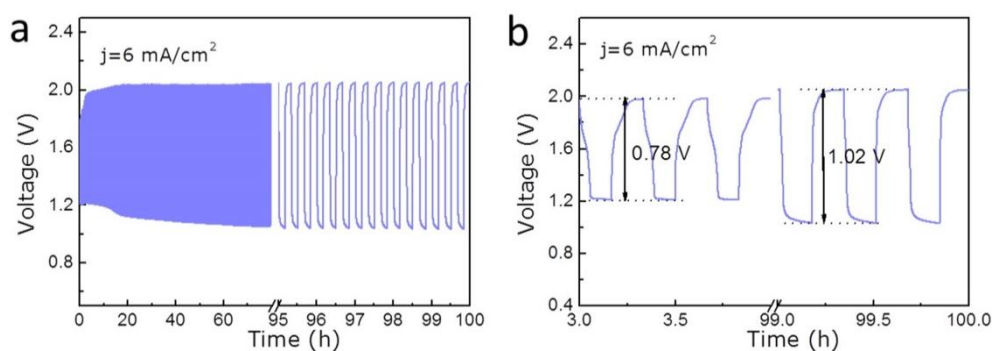


Fig. S19 **a** Galvanostatic discharge-charge cycling curves at 6 mA cm⁻² of the rechargeable Zn-air battery. **b** Charge discharge efficiency at the beginning and final of Zn-air battery at 6 mA cm⁻²

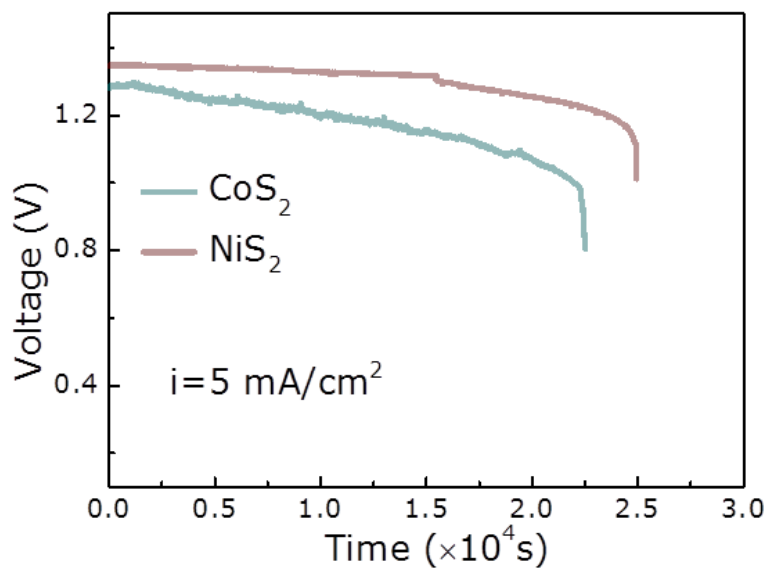


Fig. S20 Long-time discharge curves of NiS₂ and CoS₂ Zn-air battery at 5 mA cm⁻²

S10 Turnover Frequency (TOF) in HER Calculation

Voltammetric charges (Q) is calculated by the following equation [S4]:

$$Q = 2Fn$$

Where F is Faraday constant ($96,480 \text{ C mol}^{-1}$), n is the number of active sites. The factor 2 suggests that the formation of one hydrogen molecule needs two electrons in HER. In the experiment, the voltammetry curve is obtained by CV measurements with phosphate buffer ($\text{pH} = 7$) at a scan rate of 50 mV s^{-1} . When the number of voltammetric (Q) is obtained after deduction of the blank value.

The turnover frequency (TOF) can be calculated with the following equation:

$$\text{TOF} = I/Q$$

Where $I(\text{A})$ is the current of the polarization curve, we obtained it from the LSV measurements.

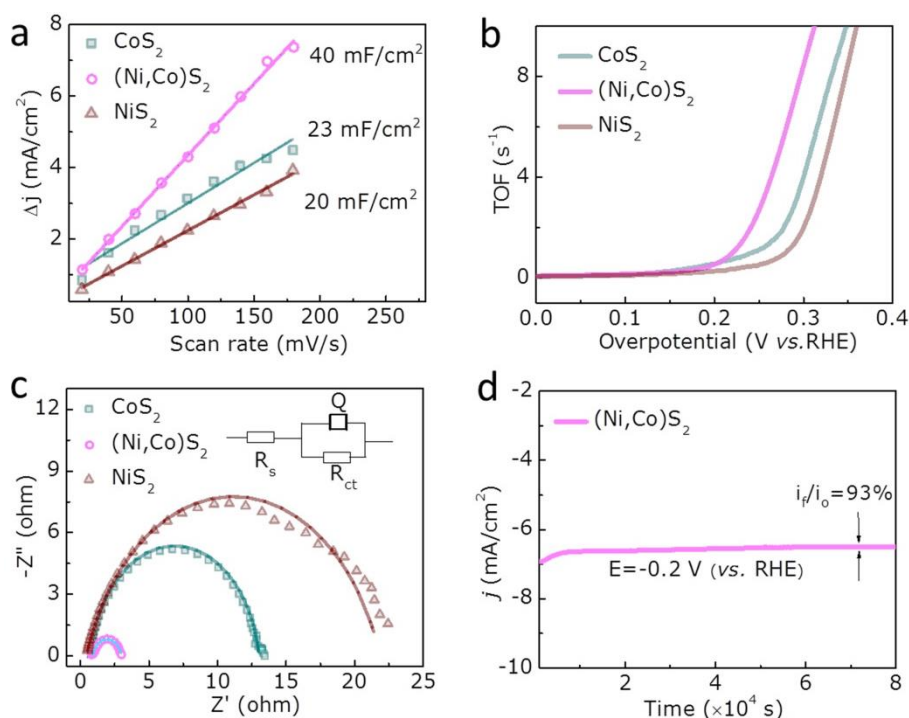


Fig. S21 **a** The C_{dl} obtained via cyclic voltammetry at different scan rates. **b** The TOF of $(\text{Ni,Co})\text{S}_2$, NiS_2 and CoS_2 . **c** EIS of $(\text{Ni,Co})\text{S}_2$, NiS_2 and CoS_2 , the insert is analogue circuit diagram. **d** The $i-t$ curve of $(\text{Ni,Co})\text{S}_2$ at -0.2 V vs. RHE for $8 \times 10^4 \text{ s}$

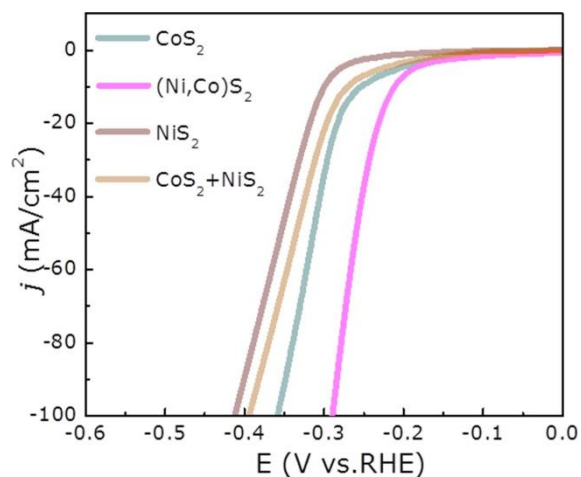


Fig. S22 HER polarization curves of (Ni,Co)S₂, NiS₂, CoS₂ and (CoS₂+NiS₂) at 5 mV s⁻¹ in 0.1 M KOH

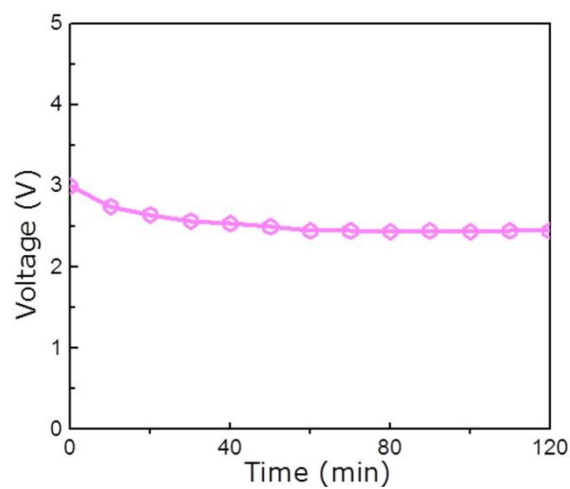


Fig. S23 Time dependence of the Voltage measured by multimeter in the self-driven overall water-splitting unit

Table S1 Comparison of OER performance for catalysts studied and Ir/C

Catalysts	Onset potential [V vs. RHE]	η at $J = 10$ mA cm ⁻² [mV]	Tafel slope [mV dec]	C_{dl} [mF cm ⁻²]	TOF at $\eta=1.55$ V [s ⁻¹]
(Ni,Co)S ₂	240	270	58	41	3.02
NiS ₂	340	410	123	16	0.22
CoS ₂	270	350	107	30	0.65
Ir/C	250	310	77	-	-

Table S2 Comparison of OER performance for previous catalysts

Catalysts	Onset potential [V vs. RHE]	η at $J = 10$ mA cm ⁻² [mV]	Tafel slope [mV/dec]	Stability [h]	References
(Ni,Co)S₂	240	270	58	19.4	This work
CoNi LDH/CoO-1	250	300	123	36	[S5]
NG-NiCo	350	-	614	12	[S6]
Ni _x Co _{3-x} O ₄ NWs	500	-	59	-	[S7]
CoNi(OH) _x	250	280	77	24	[S8]
NiCoFe-LDH	-	265	98	30	[S9]
NiCoMnO ₄ /N-rGO	270	520	128	3	[S10]
NiCo ₂ O ₄ /NF	-	-	135	10	[S11]
(NiCo)S/OH	-	227	77.5	-	[S12]
Fe-NiCo ₂ O ₄	245	302	42	10	[S13]
Ni _{0.5} Co _{0.5} S ₂	-	-	61	4	[S14]
Ni _{0.13} Co _{0.87} S _{1.097}	262	316	54.7	2	[S15]

Table S3 Comparison of ORR performance for catalysts studied

Catalysts	Onset potential [V vs. RHE]	Half-wave potential $E_{1/2}$ [V vs. RHE]	Cathodic peak at O ₂ -saturated [V vs. RHE]	Limiting current density [mA cm ⁻²]	Electron transfer number (n)
(Ni,Co)S ₂	0.82	0.71	0.75	4.2	3.98
NiS ₂	0.76	0.68	0.74	3.7	2.21
CoS ₂	0.79	0.63	0.67	3.2	2.14